2013 American Control Conference (ACC)
Washington, DC, USA, June 17-19, 2013

Design of a Constant Force Clamp and Estimation of Molecular Motor Motion using Modern Control Approach

Subhrajit Roychowdhury, Shreyas Bhaban, Srinivasa Salapaka, Murti Salapaka

Abstract— **Since its inception, optical traps have become an important tool for single molecule investigation because of its precise ability to manipulate microparticles and probe systems with a force resolution of the order of fN. Its use as a constant force clamp is of particular importance in the study of molecular motors and DNA. The highly nonlinear nature (specially the presence of hysteresis) of the force-extension relationships in such biomolecules is traditionally modelled as a linear Hookean spring for small force perturbations. For these linear models to hold, high disturbance rejection bandwidths are required so that the perturbations from the regulated values remain small. The absence of systematic design and performance quantification in the current literature is addressed by designing an optimized PI and a $\mathbf{H}_\infty$ controller, that significantly improve the force regulation and its bandwidth. A major application of constant force clamps is in step detection of biomolecules, where due to the presence of thermal noise, one has to extract the stepping data via postprocessing. In this paper, a real time step-detection scheme, currently lacking in literature, is achieved via a mixed objective $\mathbf{H_2}/\mathbf{H}_\infty$ synthesis. In the design, the $\mathbf{H}_\infty$ norm for force regulation and stepping estimation error is minimized while keeping the $\mathbf{H_2}$ norm of the thermal noise on the stepping estimate is kept bounded.**

Keywords: Constant force clamp, isotonic clamp, kinesin stepping, real time step detection, mixed objective $\mathbf{H_2}/\mathbf{H}_\infty$ synthesis, optical trap.

I. Introduction

Engineering concepts have an important role to play in biophysical research where there is an urgent need for faster instruments for single-molecule studies to understand the mechanism of motor-protein based intracellular transport at native cellular condition. Motor proteins, such as kinesin and dynein, serve as carriers for cellular cargo in intracellular transport that influence global aspects of cell biology including establishment of cell polarity, maintenance of genomic stability, regulation of higher brain functions, developmental patterning and suppression of tumorigenesis. Malfunctions in intracellular transport underlie a host of medical maladies including neurodegenerative diseases such as Alzheimers [7], [12].

The challenge in gleaning information about motor protein dynamics arises from the requirements of nm spatial resolution, second to millisecond temporal resolution, high degree of thermal noise and the fragility of the bio-matter (requires very small probing force). Optical tweezers, a laser based probing system, are uniquely positioned to address these challenges because of their capability to probe systems with fN force resolution and detect events with nm spatial resolution [6]. Typically, the motor proteins are decorated with a polystyrene bead which is then probed by the laser trap to interrogate various aspects of the motor protein dynamics indirectly.

In many in-vitro experimental scenarios, it is important for the biologists to keep the load force constant on the bead despite external disturbances (such as motor stepping, unfolding of domains and thermal force). This would allow them to simulate and study the in-vivo condition of constant load force on the molecule while avoiding complications arising due to the nonlinear nature of the force-extension relationship of the biomolecule under tension. Also, constant load eliminates the need for linkage corrections to infer displacement information of the bio-molecule attached from the position of the bead [13].

The existing force clamps can be broadly divided into two categories: active clamps and passive clamps. Active clamps [13], [8] employ feedback to move the trap location such that a preset distance between the trap location and the center of the trapped bead (and hence a preset force on the bead) is maintained, whereas in passive clamps [10], [5] the trapped bead is placed in a constant force region of the trapping potential. The main drawback of existing active clamps [13], [8] is their slow disturbance rejection bandwidth and occasional instability, which stems from neglecting the instrument dynamics and lack of formal controller design methodology. The passive clamps on the other hand, despite their higher bandwidth, is not suitable

978-1-4799-0178-4/$31.00 ©2013 AACC

for fast moving motor proteins due to reduced trapping force [10] and limited extent of constant force region [5].

In this paper we circumvent the aforementioned problems by employing modern control techniques and by precisely characterizing the instrument dynamics. A H_2/H_∞ mixed objective controller synthesis is also applied to estimate the stepping motion in real time as well, where H_∞ synthesis alone are shown to be insufficient.

II. Modelling, Characterization and Design Objectives

A. Physical Model

An optically trapped bead carried by a molecular motor in a fluid can be modeled as a spring mass damper system. Let x_T, x_b and x_m denote the positions of the trap center, bead centre and the motor head on the microtubule respectively and β represents the visocus damping coefficient. The trap and the motor are assumed to act as linear Hookean springs with respective stiffnesses k_T and k_m, under the assumptions that the excursions of $|x_T - x_b|$ and $|x_m - x_b|$, or the magnitude of corresponding forces f_T and f_m remain small at all times. The validity of this constraint is ensured by imposing appropriate design constraints. Also, we ignore any geometric effects due to the finite size of the bead.

The system is highly overdamped [2], [11] and hence the equation of motion of the bead in presence of thermal noise η is written as,

$$\beta \dot{x}_b = k_T(x_T - x_b) + k_m(x_m - x_b) + \eta. \quad (1)$$

After taking Laplace trasform and rearranging, we get,

$$x_b(s) = G(s)(k_T x_T(s) + k_m x_m(s) + \eta(s)) \quad (2)$$

where $G(s) = \frac{1}{\beta s + k_T + k_m}$.

B. Instrumentation Dynamics

The control hardware and actuation system dynamics significantly affect the overall system [2], [11] and thus should be included for a good control design. We introduce the transfer function $D(s)$ to represent the instrumentation dynamics, *i.e.,* change in trap position $x_T(s) = D(s)u(s)$ for a trap movement command $u(s)$. Thus, in absence of any motor force f_m and thermal noise, for a given command u, the measured bead position in open loop is governed by the equation,

$$\tilde{x}_b(s) = x_b(s) + n(s) = k_T G_p(s) D(s) u(s) + n(s). \quad (3)$$

where n is the measurement noise and $G_p(s) = \frac{1}{\beta s + k_T}$.

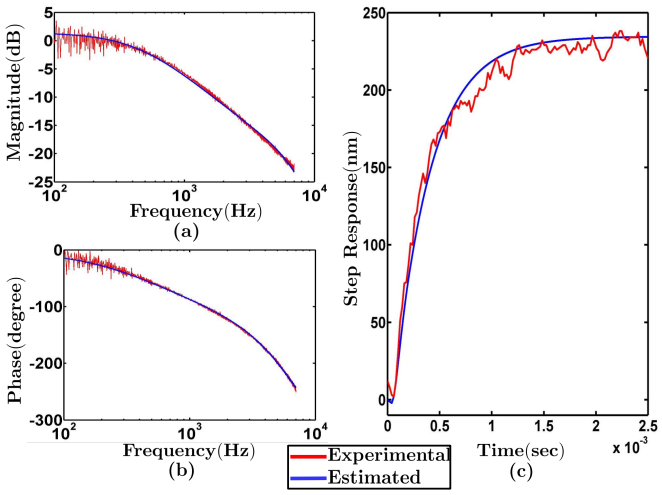

Fig. 1. (a) Magnitude response and (b) phase response of an optically trapped bead including the instrumentation dynamics. The red curve represents the experimentally obtained responses while the blue curve corresponds to those of a 2-zero, 3-pole fit of the experimental data. (c) Validation of the estimated transfer function by comparing the experimental (in red) and simulated step response (in blue).

C. System Characterization

The parameters of the physical system estimated by power spectrum method [11] yielded $\beta = 4.721 \times 10^{-6}$ pNs/nm and $k_T = 0.05$ pN/nm. To estimate $D(s)$, we give a chirp input with frequency varying from 10 Hz - 10000 Hz to the system. By fitting a 2-zero, 3-pole transfer function to the experimentally obtained frequency response data, the transfer function from control effort u to $\tilde{x}_b$ is estimated as $H(s) = k_T G_p(s) D(s) = \frac{712.3(s-1.431\times10^5)(s-5.123\times10^4)}{(s+2852)(s^2+5.317\times10^4 s+1.561\times10^9)}$. The transfer function is validated by matching experimentally obtained frquency response data and step responses to those of the estimated system (see Fig. 1). From the estimated $H(s)$, $D(s)$ is estimated as $D(s) = \frac{0.067255(s-1.431\times10^5)(s-5.123\times10^4)(s+1.059\times10^4)}{(s+2852)(s^2+5.317\times10^4 s+1.561\times10^9)}$.

D. Design Objectives

A block diagram representing the optical trap with the feedback system is shown in Fig. 2(a). The requirements of a good isotonic clamp with an additonal objective of estimation of motor motion is summarized below in terms of design objectives. For the sake of simplicity, we use H to denote any transfer function $H(s)$, and any transfer function from input a to output b is denoted by T_{ab}.

- A small value of $\|T_{x_m e_F}\|_{H_\infty}$ would ensure that the motor stepping motion does not significantly alter the force on the system, which is the main objective of the isotonic clamp. Here e_F denotes

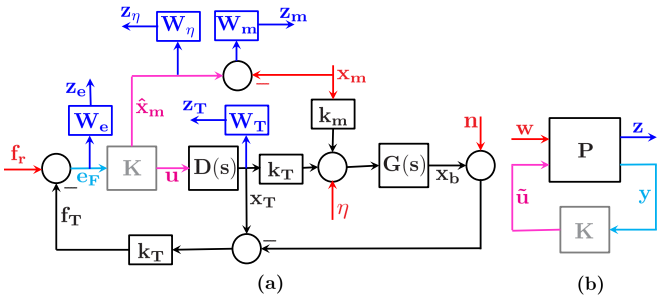

Fig. 2. (a) The block diagram showing different inputs, disturbances, weighted fictitous outputs, measured signals and control signals. Here the main aim is to obtain an estimate $\hat{x}_m$ of motor motion x_m while maintaining the force f_m on the motor regulated at a constant value f_r. The influence of thermal noise η needs to be small on the estimate $\hat{x}_m$ and the actuator effort x_T should be limited to avoid losing the bead from the trap. (b) The modern control design framework showing the plant P, controller K, exogenous input vector w, weighted signal vector z, measured signal vector y and control signal vector $\tilde{u}$.

the force regulation error, the difference between the desired force f_r to be maintained on the molecule and the trap force f_T. The desired bandwidth of force regulation is captured in z_e by the corresponding weighting function W_e.

- For good command tracking, we need $\|T_{f_r e_F}\|_{H_\infty}$ to be small.
- For good estimation of motor motion, $\|T_{x_m \tilde{x}_m}\|_{H_\infty}$ should be small, where $\tilde{x}_m = \hat{x}_m - x_m$ denotes the error in estimation of motor motion. z_m captures the desired bandwidth of estimation through W_m.
- Small $\|T_{\eta \hat{x}_m}\|_{H_2}$ ensures reduced effect of thermal noise on the estimate of the motor motion. z_η captures the desired range of filtering via W_η.
- To avoid losing the bead from the trap due to sudden spikes in trap position, we require $\|T_{x_m x_T}\|_{H_\infty} \leq 1$, as that would ensure that the input disturbance is not magnified to the trap position. Also, for the linearity assumptions to hold good, trap movement should be small. This constraint takes care of the actuator saturation as well, which has a much higher limit.
- Any controller should be robust enough to endure certain variation of the motor spring constant k_m.
- The measurement noise in similar systems [2] is observed to be substantially below the thermal noise response and thus is not considered under the design objectives.

It can be seen that the requirements for different objectives are conflicting and thus all of them can not be satisfied simultaneously for all frequencies. In the following sections we present LMI-based control design methodology where the resulting controller optimizes certain objective transfer functions while guaranteeing practical bounds on values of other transfer functions (where these objectives can be characterized by H_2 or H_∞ norms on the transfer functions). We present and solve a few such optimal control problems each of which reflects a specific experimental scenario and objective.

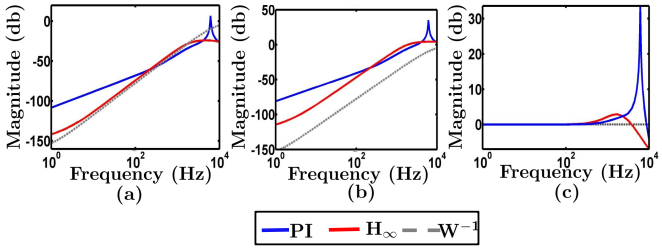

Fig. 3. Comparison of performances from frequency responses between the PI controller (shown in blue) and the H_∞ controller (shown in red) for different performance objectives : (a) $\|T_{x_m e_F}\|$ and $\|W_e^{-1}\|$ (b) $\|T_{f_r e_F}\|$ and $\|W_e^{-1}\|$ (c) $\|T_{x_m x_T}\|$ and $\|W_T^{-1}\|$. The inverse of weighting function is shown in gray.

III. Design of a Constant Force Clamp

In this section, we design controllers for constant force clamps that would have good error regulation (small $\|T_{x_m e_F}\|_{H_\infty}$) and good command tracking (small $\|T_{f_r e_F}\|_{H_\infty}$) in closed loop. We first design a PI controller and then a H_∞ controller to show improvment in performance over the former. For the H_∞ design, we incorporate an additional objective of avoiding amplification of input disturbances at the actuator output (small $\|T_{x_m x_T}\|_{H_\infty}$) to avoid losing the bead during experiment.

A. PI controller

By using loop shaping techniques, we obtain a PI controller as $K_{PI}(s) = k_p(1 + \frac{1}{T_i s})$, where $K_p = 58.5$ and $T_i = 4.1667 \times 10^{-5}$ s. The frequency plots and simulation results in Fig. 3 and Fig. 4 shows the closed loop system with PI controller to have good command tracking and error regulation for a reasonable bandwidth.

B. H_∞ controller

Design: To meet the specified performance objectives,we choose $z = [z_e \; z_T]^T$, $w = [x_m \; f_r]^T$, $\tilde{u} = u$ and $y = e_F$ (see Fig. 2(a)), making our generalized

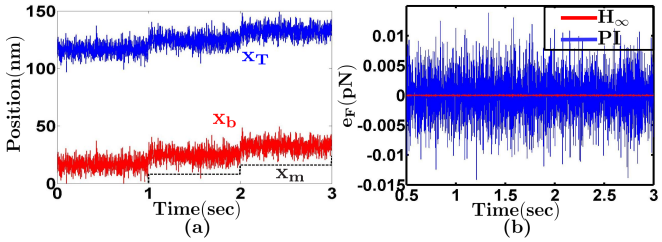

Fig. 4. Simulation results: (a) Change in bead position x_b (shown in red) and the corresponding control effort x_T (shown in blue) in response to input step disturbances x_m of amplitude 8 nm (shown in black) with the H_∞ controller in presence of input noise η with $\sigma_{noise} = 5$ pN. (b) Regulation error e_F with the PI controller (shown in blue) and that with the H_∞ controller (shown in red) in presence of the aforementioned input disturbance and noise for $f_r = 5$ pN.

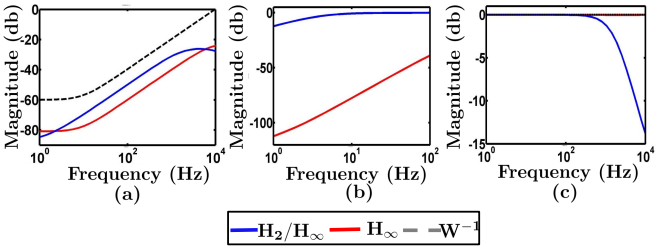

Fig. 5. Comparison of performances from frequency responses between the H_2/H_∞ mixed objective controller (shown in blue) and the H_∞ controller (shown in red)for different performance objectives : (a) $\|T_{x_m e_F}\|$ and $\|W_e^{-1}\|$ (b) $\|T_{x_m \tilde{x}_m}\|$ (c) $\|T_{x_m x_T}\|$ and $\|W_T^{-1}\|$. The inverse of weighting function is shown in gray.

open loop plant from $[w \mid \tilde{u}]^T$ to $[z \mid y]^T$ to be

$$P = \left[\begin{array}{cc|c} W_e k_T k_m G & W_e & -W_e k_T D(1 - k_T G) \\ -W_T k_m G & 0 & W_T D(1 - k_T G) \\ \hline k_T k_m G & 1 & -k_T D(1 - k_T G) \end{array}\right] \quad (4)$$

Our objective is to design a stabilizing controller K that would minimize $\|\Psi\|_{H_\infty}$, where Ψ is the closed loop transfer function from w to z (see Fig. 2(b)). We use the performance of the PI controller as a guideline for choosing W_e. The choice of W_T is dictated by the fact that we want to avoid amplification of disturbance x_m at x_T.

Performance: The frequency plots in Fig. 3 show improvements in terms of command tracking and error regulation when compared to those of the PI controller. The simulation results in Fig. 4(b) and in the following table also corroborate the same.

From the frequency plots (Fig. 3) and the simulation results (Fig. 4(b)), the H_∞ controller clearly outperforms the PI controller for an isotonic clamp in every aspect. Frequency plots with the PI controller shows peaks at high frequencies (see Fig. 3) which can be explained from second waterbed theorem and the presence of RHP zeros in the system [11], [2]. This emergence of peaks poses a bottleneck on the resolution and bandwidth that can be achieved, and modern control design is seen to push that limit much further when compared to traditional design by eliminating those peaks at operating frequencies. The elimination of the huge peak in the $\|T_{x_m x_T}\|$ via modern control design (see Fig. 3(c)) worths special mentioning, as it eliminates the possibility of getting an experiment hampered due to the loss of the bead from the trap due to the amplification of a sudden disturbance spike at the input.

Another major advantage obtained via H_∞ synthesis is that of robustness. For the PI controller, the system performance degrades as the value of the uncertain parameter k_m is increased from its nominal value of 0.3 pN/nm, making it unstable for $k_m = 0.375$. The H_∞ controller, however, shows little degradation in performance till k_m is increased to a value of 0.5 pN/nm, much above of what is to be expected in an isotonic clamp operation.

IV. Estimation of Molecular Motor Motion

As already mentioned, an important application of isotonic clamp is in the detection and estimation of molecular motor motion. The bead motion is assumed to follow the motor motion at steady state if constant force is maintained. As an alternative to the existing scheme of x_m detection, we design our controller to directly give an estimate of x_m, which would enable us to detect steps in real time. We first design a H_∞ controller and point out its defficiencies for the purpose. We then circumvent them by designing a mixed objective H_2/H_∞ controller.

A. $\mathbf{H_\infty}$ controller

The H_∞ controller is designed to have good force regulation (small $\|T_{x_m e_F}\|_{H_\infty}$), good estimation of motor motion (small $\|T_{x_m \tilde{x}_m}\|_{H_\infty}$) and avoiding amplification of input disturbances at the actuator output (small $\|T_{x_m x_T}\|_{H_\infty}$). Although the frequency plots show good error regulation and good bandwidth for x_m estimation (Fig. 5(b) shows the frequency plot for estimation error), the results(Fig. 6(c) and Fig. 7(c)) reveal that $\hat{x}_m$ is highly corrupted with noise (specially for high noise level with $\sigma_{noise} = 10$ pN), rendering the estimate ineffective for real time step detection.

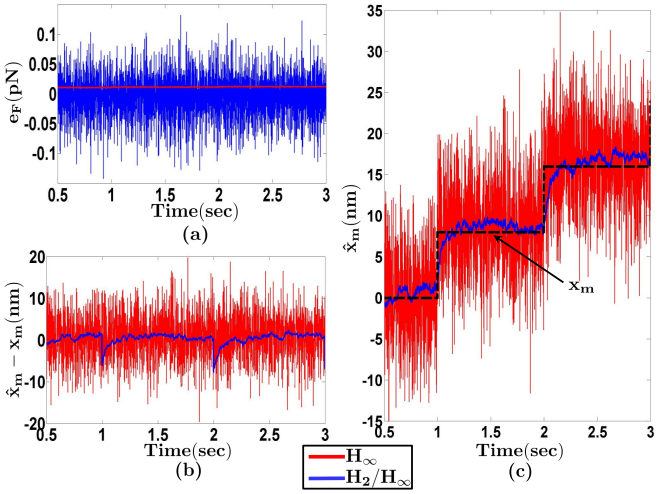

Fig. 6. Comparison of performances from simulation results between the H_2/H_∞ mixed objective controller (shown in blue) and the H_∞ controller (shown in red) for low thermal noise ($\sigma_{noise} = 5$ pN) and $f_r = 5$ pN: a) Error in force regulation. (b) Error in step estimation. (c) Estimate of steps.

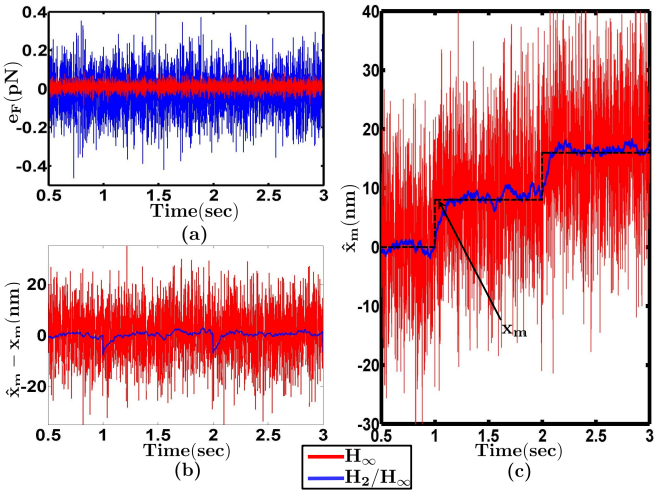

Fig. 7. Comparison of performances from simulation results between the H_2/H_∞ mixed objective controller (shown in blue) and the H_∞ controller (shown in red) for high thermal noise ($\sigma_{noise} = 10$ pN) and $f_r = 5$ pN: (a) Error in force regulation. (b) Error in step estimation. (c) Estimate of steps. Here a tigher bound on $\|\Psi_2\|_{H_2}$ is imposed by sacrificing $\|\Psi_\infty\|_{H_\infty}$ to some extent to counter the increased noise level.

B. Mixed objective H_2/H_∞ controller

Design: We argue that to reduce the effect of input noise on $\hat{x}_m$, $\|T_{\eta\hat{x}_m}\|_{H_2}$ should be small. As η and x_m comes at the same input (see Fig. 2(a)), making $\|T_{x_m\hat{x}_m}\|_{H_2}$ small serves the same purpose while making the design process much simpler. To incorporate this additional objective in the mixed objective design framework, we define $z_\infty = [z_e \ z_m \ z_T]^T$, $z_2 = z_\eta$, $z = [z_\infty \ z_2]^T$, $w = x_m$, $\tilde{u} = [u \ \hat{x}_m]^T$ and $y = e_F$ (see Fig. 2(a)), making our generalized open loop plant from $[w \mid \tilde{u}]^T$ to $[z \mid y]^T$ as

$$P = \left[\begin{array}{cc|c} W_e k_T k_m G & -W_e k_T D(1-k_T G) & 0 \\ -W_m & 0 & W_m \\ -W_T k_m G & W_T D(1-k_T G) & 0 \\ 0 & 0 & W_\eta \\ \hline k_T k_m G & -k_T D(1-k_T G) & 0 \end{array}\right] \quad (5)$$

Our objective is to design a stabilizing controller K that would minimize $\|\Psi_\infty\|_{H_\infty}$, subject to $\|\Psi_2\|_{H_2} < \nu$. Here Ψ_∞ and Ψ_2 are the transfer functions of the closed loop channels from w to z_∞ and z_2 respectively. Ψ_∞ and Ψ_2 are in turn obtained from Ψ, the closed loop transfer function from w to z. Choice of W_m is dictated by the fact that as $\hat{x}_m$ is needed at steady state, we do not need high bandwidth of estimation, as long as the error regulation bandwidth is high enough to validate linearity assumptions, which in turn dictates the choice of W_e.

Performance: Frequency plots for the mixed objective controller show good enough error regulation bandwidth for the linearity assumptions to hold good (Fig. 5(a)). The x_m estimation bandwidth however decreases considerably than the previous case (Fig. 5(b)), which is to be expected as we are decreasing the H_2 norm over the same channel. A trade-off is achieved through the choice of different weighting functions. Simulation results show (Fig. 6(c) and Fig. 7(c))that this bandwidth is good enough to get a clean estimate of x_m even for high noise levels. Although the force regulation deteriorate, it is still better ($< 2\%$) than that reported in [14] (10%) for similar noise level. Even with higher noise level, we achieve better force regulation($< 5\%$), and thus the linearity assumptions can be assumed to hold good for all practical purposes with the mixed objective controller.

V. Conclusion

The paper presents real life applications of H_∞ and mixed objective H_2/H_∞ controller synthesis and discusses various design trade-offs among them. The currently lacking systematic design for constant force clamp design [14], [9] is addressed via a modern control design methodology. Significant improvement in force regulation and operational bandwidth is achieved by the understanding of fundamental limitations on achievable performance due to presence of RHP zeros. Modern control design framework is successfully employed to overcome those limitations within operating range of frequencies. This improvement in bandwidth

and resolution[1] may have a greater impact on biomolecular studies, as this will enable the scientists to discover events not previously possible, thereby refining the existing models. Better force regulation over a higher a bandwidth also validates the linearity assumptions with higher confidence. Modern control design makes the system robust against possible variations of uncertain experimental parameters as well.

The paper also develops a *real time* step detection scheme for molecular motors, which to the best of the author's knowledge has not been addressed so far in the current literature. This can be of immense importance to experimental biologists, as they will be able to detect motility in the sample at a very early stage of the experiment when compared to the currently existing postprocessing schemes of step detection [3], [1]. The real time step detection scheme is attained by mixed objective H_2/H_∞ synthesis, where the effect of brownian noise on the estimate is decreased by keeping the H_2 norm of the channel bounded, while we minimize the H_∞ norm over the estimation error and error regulation channels. This scheme avoids influencing the system being probed and thus preserving normal system dynamics, unlike certain other schemes of reduction of influence of thermal noise by stiffeing the system itself [4].

Note that the bandwidth of estimation for the real time scheme is limited to a few Hz (see Fig. 3(b)), which is a result of the H_2/H_∞ trade-off over the same channel. From simulations, this bandwidth is seen to be good enough for low motor velocities (typically around $30 - 40$ nm/s for kinesin) for typical noise levels ($\sigma_{noise} = 5pN$), which corresponds to low ATP concentration and high load force scenarios[15]. This can possibly be improved by exploiting the noise properties to select the weighting function W_η more effectively and minimizing only $\|T_{x_m\tilde{x}_m}\|_{H_\infty}$ subject to appropriate bounds on other H_2/H_∞ norms of other channels, which would allow for better allocation of controller efforts.

REFERENCES

[1] Tanuj Aggarwal, Donatello Materassi, Robert Davison, Thomas Hays, and Murti Salapaka. Detection of steps in single molecule data. *Cellular and Molecular Bioengineering*, 5:14–31, 2012. 10.1007/s12195-011-0188-5.

[2] Tanuj Aggarwal, Hullas Sehgal, and Murti Salapaka. Robust control approach to force estimation in a constant position optical tweezers. *Review of Scientific Instruments*, 82(11):115108 –115108–9, nov 2011.

[3] Steven M. Block. Kinesin motor mechanics: Binding, stepping, tracking, gating, and limping. *Biophysical Journal*, 92(9):2986 – 2995, 2007.

[4] J.J. Gorman, A. Balijepalli, and T.W. LeBrun. Feedback control of optically trapped particles. *Feedback Control of MEMS to Atoms*, pages 141–177, 2012.

[5] William J Greenleaf, Michael T Woodside, Elio A Abbondanzieri, and Steven M Block. Passive all-optical force clamp for high-resolution laser trapping. *Physical review letters*, 95(20):208102, 2005.

[6] William J Greenleaf, Michael T Woodside, and Steven M Block. High-resolution, single-molecule measurements of biomolecular motion. *Annual review of biophysics and biomolecular structure*, 36:171, 2007.

[7] N. Hirokawa, Y. Noda, Y. Tanaka, and S. Niwa. Kinesin superfamily motor proteins and intracellular transport. *Nature Reviews Molecular Cell Biology*, 10(10):682–696, 2009.

[8] Matthew J Lang, Charles L Asbury, Joshua W Shaevitz, and Steven M Block. An automated two-dimensional optical force clamp for single molecule studies. *Biophysical journal*, 83(1):491–501, 2002.

[9] Matthew J. Lang, Charles L. Asbury, Joshua W. Shaevitz, and Steven M. Block. An automated two-dimensional optical force clamp for single molecule studies. *Biophysical Journal*, 83(1):491 – 501, 2002.

[10] Rajalakshmi Nambiar, Arivalagan Gajraj, and Jens-Christian Meiners. All-optical constant-force laser tweezers. *Biophysical journal*, 87(3):1972–1980, 2004.

[11] H. Sehgal, T. Aggarwal, and M.V. Salapaka. Systems approach to identification of feedback enhanced optical tweezers. In *Proceedings of SPIE*, volume 7038, page 703821, 2008.

[12] Gorazd B Stokin, Concepción Lillo, Tomás L Falzone, Richard G Brusch, Edward Rockenstein, Stephanie L Mount, Rema Raman, Peter Davies, Eliezer Masliah, David S Williams, et al. Axonopathy and transport deficits early in the pathogenesis of alzheimer's disease. *Science*, 307(5713):1282–1288, 2005.

[13] Koen Visscher and Steven M Block. [38] versatile optical traps with feedback control. *Methods in enzymology*, 298:460–489, 1998.

[14] Koen Visscher and Steven M. Block. [38] versatile optical traps with feedback control. In Richard B. Valee, editor, *Molecular Motors and the Cytoskeleton Part B*, volume 298 of *Methods in Enzymology*, pages 460 – 489. Academic Press, 1998.

[15] Koen Visscher, Mark J. Schnitzer, and Steven M. Block. Single kinesin molecules studied with a molecular force clamp. *Nature*, 400:184–189, 1999.

[1]Better regulation will give better resolution, as systems can be probed in steps of smaller intervals of force values.